Journal of Luminescence 148 (2014) 111–115

Contents lists available at ScienceDirect

Journal of Luminescence

journal homepage: www.elsevier.com/locate/jlumin

Preheating-temperature effect on structural and photoluminescent properties of sol–gel derived ZnO thin films

C.H. Chia [a,*], W.C. Tsai [a], W.C. Chou [b]

[a] Department of Applied Physics, National University of Kaohsiung, Kaohsiung 81148, Taiwan
[b] Department of Electrophysics, National Chiao Tung University, Hsinchu 30010, Taiwan

ARTICLE INFO

Article history:
Received 30 August 2013
Received in revised form
30 November 2013
Accepted 5 December 2013
Available online 14 December 2013

Keywords:
ZnO
Sol–gel
Photoluminescence
Exciton

ABSTRACT

We investigated the evolution of structural and low-temperature photoluminescence properties of sol–gel derived ZnO thin films, as a function of pre-heating temperature between 300 °C and 600 °C. The pre-heating crystallization plays an important role in the lineshape of PL spectra. The increase in pre-heating temperature enables rearrangement of atoms at the pre-heating stage, leading to *c*-axis oriented growth of films, modification in lineshape of impurity-defect emission, and reduction of deep-level emission intensity.

1. Introduction

ZnO thin films show a versatile combination of interesting optical, electrical and magnetic properties [1]. Consequently, this material has been attracting great attention due to its potential applications in ultra-violet optoelectronics devices [2,3], solar cells [4], thin film transistors [5], gas sensors [6], and surface acoustic wave devices [7] and so on. In particular, wide band gap (3.37 eV) at room-temperature (RT) and large exciton binding energy (60 meV) [1] of ZnO enable the utilization of exciton-related transitions in ultra-violet light-emitting devices even at RT. It is therefore a promising semiconductor for photonics applications such as polariton lasers [8] and microcavity-based devices [9].

Sol–gel technique is much cheaper and easier to grow large area of ZnO films than much sophisticated techniques. The sol–gel derived ZnO thin films have already been realized in transparent *p–n* junction diodes [10] and transistors [4]. The ZnO-films synthesis by sol–gel route includes three major steps: (i) solution preparation, (ii) coating and (iii) heat treatment. These three steps involve several parameters that influence the physical properties of the films. One of them is pre-heating temperature (T_{ph}). The T_{ph} is an important factor affecting the solvent vaporization, decomposition of precursor-material, and crystallization process. Ohyama et al. [11] studied crystalline orientations of ZnO thin films, prepared by acetate solution, with T_{ph} between 200 °C and 500 °C. The authors found that T_{ph}=300 °C is the optimum condition for preferred growth of film with (0 0 2)-orientation. Kim et al. [12] also revealed that 275 °C is the optimum T_{ph} for preferred growth of film with (0 0 2)-orientation. Santos et al. [13], however, challenged low-T_{ph} growth of ZnO thin film. The authors claimed that highly *c*-axis oriented film has been obtained at T_{ph}=120 °C. Although abundant literatures have been reported [11–16], the T_{ph} effect on low-temperature photoluminescence (PL) characteristics of sol–gel derived ZnO thin film is rarely studied. Moreover, to control the crystallization process at pre-heating stage, we adopted relatively high T_{ph}, compared with the other studies [12–16]. For a large use of sol–gel derived ZnO thin film for optoelectronic devices, a better understanding of the PL mechanisms in sol–gel ZnO thin film is necessary. Some literatures have reported the PL of sol–gel derived ZnO thin films [17–20]. However, neither of them discusses the T_{ph}-effect on the luminescent properties despite of this factor playing an important role in the crystallization of ZnO.

In this letter, we studied the evolution of PL from ZnO thin film grown by sol–gel spin-coating technique, as a function of T_{ph}. The focus of the present work is investigation of structural and PL properties of the ZnO thin films. The emphasis has been given on the PL spectra of ZnO thin film, measured at low-temperature (*T*). We found that the low-*T* PL band of the ZnO thin films is characterized by the radiative recombination of donor-bound excitons and impurity-defect-related transitions. The latter transition is greatly influenced by the T_{ph}.

2. Experimental details

The ZnO thin films were grown from aqueous solution prepared using zinc nitrate hexahydrate ($Zn(NO_3)_2 \cdot 6H_2O$) as the

* Corresponding author. Tel.: +886 7 5919713; fax: +886 7 5919357.
E-mail address: chchia@nuk.edu.tw (C.H. Chia).

0022-2313/$ - see front matter © 2013 Elsevier B.V. All rights reserved.
http://dx.doi.org/10.1016/j.jlumin.2013.12.006

starting material, isopropanol as the solvent, and monoethanolamine (MEA) as the stabilizer. The molar ratio of zinc nitrate to MEA was kept at 2:1 and the molar concentration of Zn^{2+} is 0.3 mol/L. The precursor solution was mixed thoroughly with a magnetic stirrer at 50 °C for an hour until the formation of a homogenous and transparent sol, which was aged for 7 days at RT before the coating of thin films. The ZnO thin films were formed by spin-coating the sol solution on the sapphire substrate at 2000 rpm (revolutions per minute) for 15 s. After the spin-coating process, the samples were subjected to pre-heating treatment. Four samples treated at pre-heating temperature T_{ph}=300, 400, 500, 600 °C for 10 min were grown. The procedure was repeated 10 times in order to obtain desired thickness. The samples were finally annealed in air atmosphere in a furnace at T=600 °C for 2 h.

Structural properties of the films were examined by X-ray diffraction method (XRD) using a monochromatized X-ray beam CuK_α with wavelength of 0.154 nm. Field-emission scanning electron microscopy (SEM) was employed to investigate the morphological properties of the samples. The PL spectra were measured by a 32-cm-long monochromator and a charge-coupled device camera. The pump source for the low-excitation spectra was the 310 nm-line of Xenon lamp. The excitation power for the PL measurement was kept at 2 mW/cm^2. A closed cycle refrigerator was used to perform the T-dependent measurement.

3. Results and discussion

Fig. 1 shows the XRD patterns of the ZnO thin films. The pattern suggests all of the films have hexagonal wurtzite structure. Three diffraction signals with peaks located at 31.7°, 34.4° and 36.2° are attributable to (1 0 0), (0 0 2) and (1 0 1) diffraction, respectively [1]. The ZnO film of T_{ph}=300 °C is polycrystalline. As the T_{ph} increases from 300 °C to 400 °C, the (1 0 1) diffraction intensity increases abruptly. However, the film tends to orient with c-axis perpendicular to the film surface as T_{ph} reaches 500 °C. The (0 0 2) diffraction dominates the XRD spectra for the sample of T_{ph}=600 °C, indicating that the film with preferred c-axis orientation was obtained at high T_{ph}. In order to describe the preferred c-axis orientation, the relative intensities of (0 0 2) diffraction peak $I_{(2\,0\,0)}/[I_{(1\,0\,0)}+I_{(2\,0\,0)}+I_{(1\,0\,1)}]$ as a function of T_{ph} are plotted in the inset of Fig. 1. The relative (0 0 2)-diffraction intensity of the sample with T_{ph}=400 °C is smaller than that of T_{ph}=300 °C. However, the relative intensity of (0 0 2)-diffraction increases as T_{ph} exceeds 400 °C and reaches close to unity as T_{ph}=600 °C. Since the boiling points of isopropanol and MEA are 82 °C and 170 °C respectively, T_{ph} of 300 °C is adequate to vaporize the organic residuals. However, the thermal decomposition of zinc nitrate was observed to be rapid at T above 350 °C, which is the thermal decomposition-temperature of bulk zinc nitrate [21]. The film prepared at T_{ph}=400 °C, undergoes vaporization of organic solvents and thermal decomposition of zinc nitrate abruptly and simultaneously, thus, preferentially c-axis oriented crystallization is obscured [12], leading to small relative (0 0 2)-diffraction intensity. Nevertheless, further increase of T_{ph} enables atoms acquiring enough thermal energy to rearrange, resulting in c-axis oriented growth.

Fig. 2 shows the SEM image of ZnO films deposited on sapphire substrate. The microstructure of ZnO thin film transforms from particulate-like to porous plate-like as T_{ph} increases. The film of T_{ph}=300 °C is homogeneous and slightly porous with crystalline size ranging from 50 nm to 150 nm. The surface morphology changes abruptly as T_{ph} reaches 400 °C. A lot of large pores start to form in the film prepared at T_{ph}=400 °C and the degree of porosity persists up to T_{ph}=600 °C. As a result of simultaneous chemical reactions, i.e., the quick evaporation of organic components

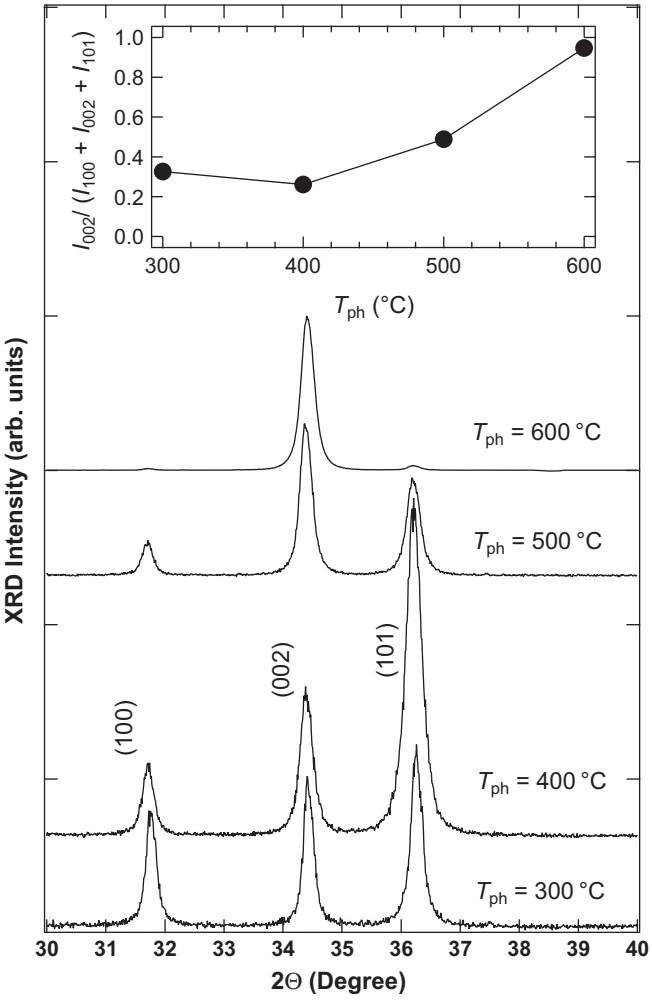

Fig. 1. XRD patterns of the ZnO thin films, as a function of T_{ph}. Three diffraction peaks corresponding to (1 0 0), (0 0 2) and (1 0 1) plane were observed. The inset shows the relative intensities of (0 0 2) diffraction peak $I_{(2\,0\,0)}/[I_{(1\,0\,0)}+I_{(2\,0\,0)}+I_{(1\,0\,1)}]$ as a function of T_{ph}.

and thermal decomposition of zinc nitrate, the pores are left behind in the films during the crystallization process. The structural and morphological changes of the precursor film prepared at T_{ph} > 400 °C, compared with that of T_{ph}=300 °C, also correlates to the PL profiles demonstrated below.

Fig. 3 reveals the normalized low-T PL spectra of the ZnO thin films prepared at various T_{ph}. Here, the low-T refers to the lowest temperature obtainable in our cryostat-system, i.e., 15 K. The radiative recombination of donor-bound exciton D°X (3.362 eV) dominates the low-T PL spectra. The chemical identity of the donor is probably the hydrogen atoms [22], which is an abundant element in our precursor-solvent. The full widths at half maximum (FWHM) of the D°X bands in all of the samples are about 7 meV, indicating good optical quality of the ZnO films. In the film of T_{ph}=300 °C, we identified an emission band located near 3.31 eV. This PL band can decompose into three radiative recombinations originated from structural defects (SD, 3.332 eV), free-to-bound transitions (eA°, 3.317 eV) and donor-acceptor pair (DAP, 3.302 eV), according to literatures [23]. The SD-band is of excitonic nature and similar to the so-called Y-line commonly seen in ZnSe and ZnTe [22]. The eA°-band is the radiative recombination of an electron from the conduction band with a hole bound to an acceptor-like defect state, caused by stacking fault [23,24]. The DAP-band is attributable to the transitions between donor and acceptor levels in the forbidden band-gap. The large amount of

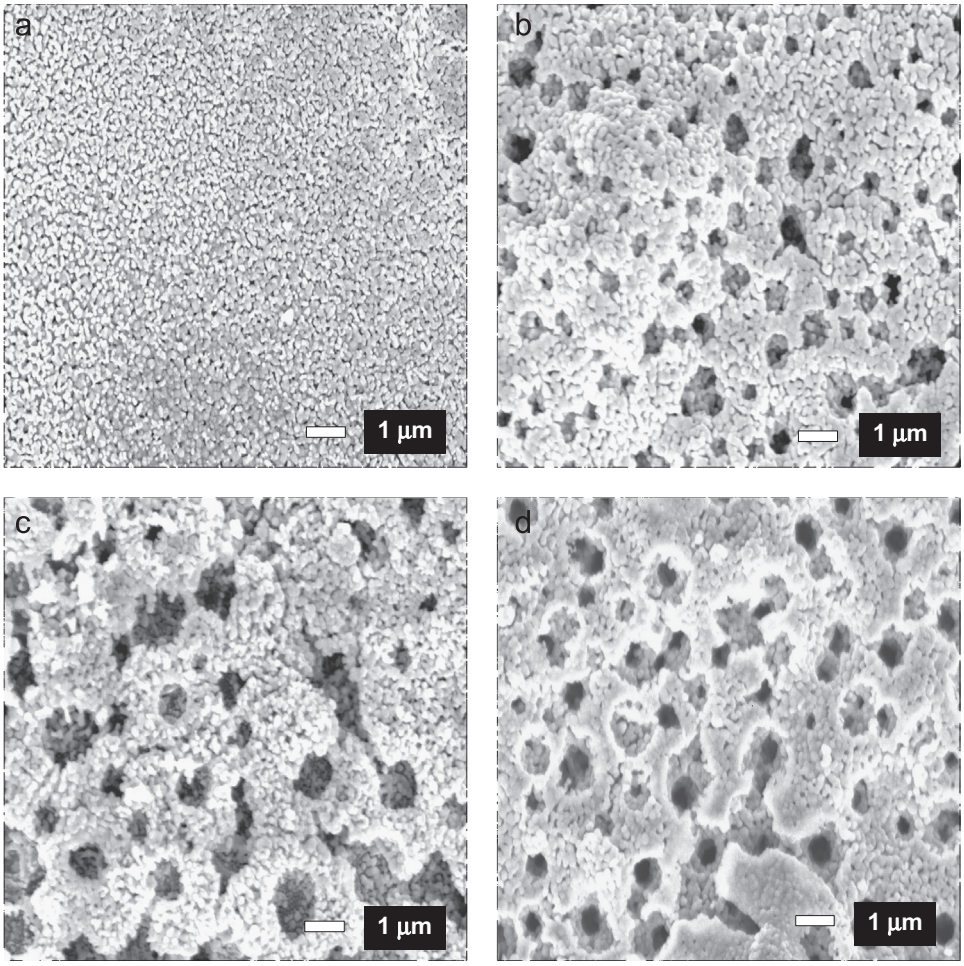

Fig. 2. FESEM images of the ZnO thin films with T_{ph} of (a) 300 °C (b) 400 °C (c) 500 °C and (d) 600 °C. The porosity becomes severe as $T_{ph} > 300$ °C.

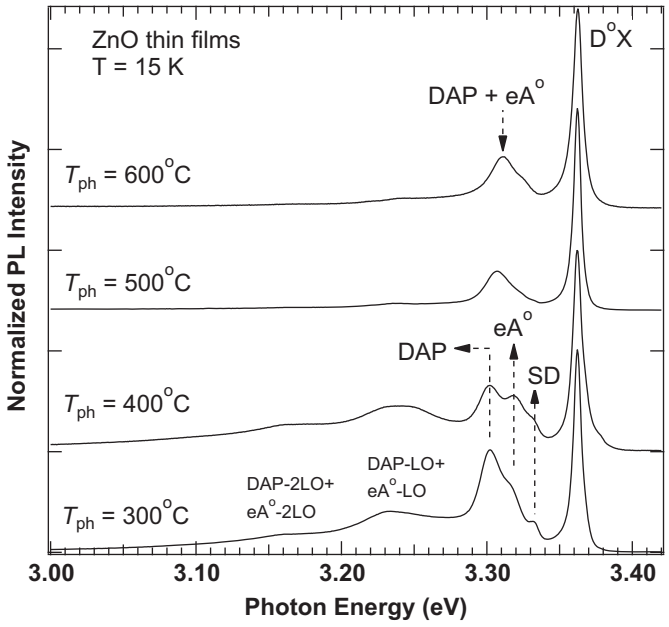

Fig. 3. Low-*T* PL spectra of the ZnO thin films, as a function of T_{ph}. The donor-bound exciton (D°X) dominates the PL spectra for all of the samples. The DAP, eA° and SD refer to donor-acceptor-pair, electron-to-bound state, and structural defect, respectively.

donors and acceptors in our samples is not surprising because of low-purity of chemical precursor materials. Small humps located at low-energy side of these emission lines are the one and two LO-phonon sideband of eA° and DAP transitions because the spectral separations between them are 72 meV and 144 meV, respectively [1]. Compared to the film of $T_{ph}=300$ °C, the intensity of eA°-band (I_{eA}) is unchanged and the intensity of DAP-band (I_{DAP}) decreases in the film of $T_{ph}=400$ °C. In addition, the intensity of SD-band I_{SD} becomes less pronounced. The decrease in I_{DAP} is simply because more impurity-atoms escape out of the film treated at high-T_{ph}. The SD-transitions originate from excitons bound to the defects induced by irregularities in the crystal [23,24]. As the irregularities disappear owing to the reconstruction of atomic arrangement under high-T_{ph}, reduction of I_{SD} is expectable. The microscopic nature of defect-states causing the eA°-transitions is rather complicated and remains unknown. However, we noted that the total impurity-defect-related emission intensity $I_{eA}+I_{DAP}+I_{SD}$ reduces as the T_{ph} increases from 300 °C to 500 °C. It has to remind that our samples were post-annealed at 600 °C. Thus, once the structural defects formed at the low-T_{ph}, they cannot be annihilated by the next post-annealing treatment. For the film with $T_{ph}=500$ °C, the SD-transitions disappear because of atomic reconstruction at the pre-heating process. The DAP and eA°-band merges into a single emission band with spectral peak about 3.308 eV. It is no doubt that the I_{eA} is smaller in the sample of $T_{ph}=500$ °C. Therefore, we can infer that the stacking faults, leading to the occurrence of eA°-transition, could also be reduced by reconstruction of atomic arrangement under high-T_{ph}. For the film with $T_{ph}=600$ °C, the emission profile is similar to that of $T_{ph}=500$ °C, except that the spectral peak of impurity-defect emission slightly blueshifts. Owing to the low-purity of precursor materials, several kinds of impurity may exist in our sample.

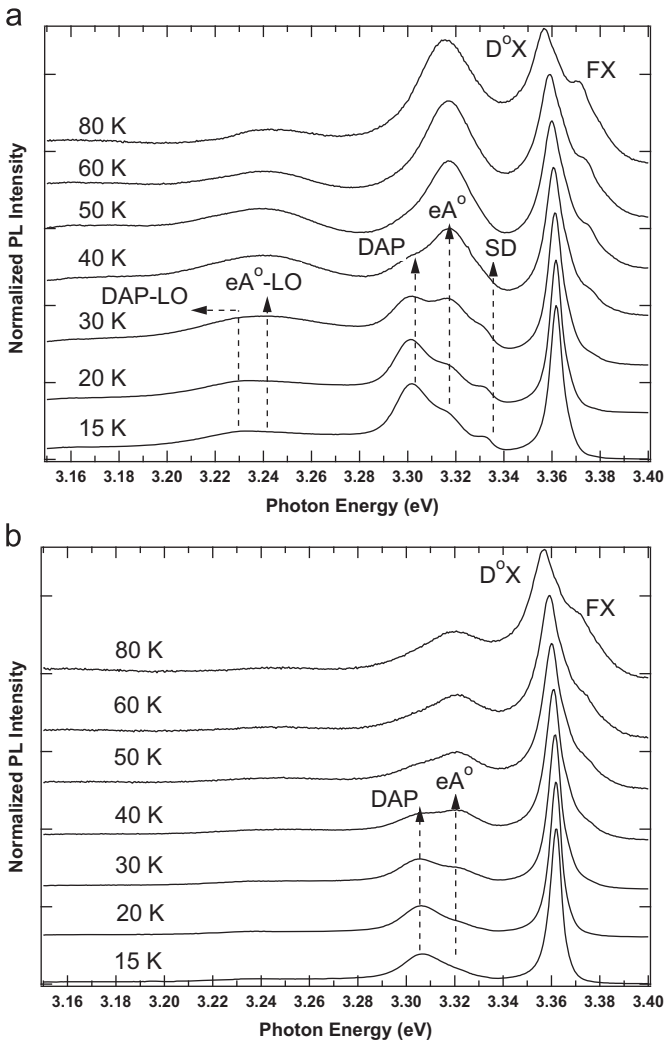

Fig. 4. *T*-dependent PL spectra of the ZnO thin films with T_{ph} of (a) 300 °C (b) 500 °C. The FX refers to free excitonic transition.

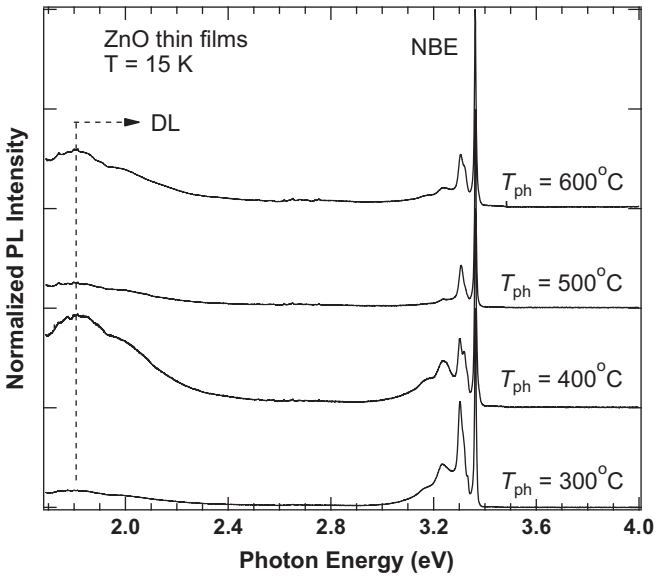

Fig. 5. Low-*T* PL spectra of the ZnO thin films measured at broad spectral range. The near-band-edge (NBE) PL is due to D°X-transitions.

Purging out of particular donors or acceptors from the film prepared at different T_{ph}, leads to energetic shifts of donor or acceptor level. This leads to changes in spectral peak of DAP-emission. As will be verified later, this single impurity-defect emission is dominated by DAP-transitions. Therefore, the change in DAP-emission peak is the major reason for the spectral difference of impurity-defect emission between the samples of T_{ph}=500 °C and 600 °C.

To get further insight about the impurity-defect-related emissions from the films, we performed *T*-dependent PL measurement. Fig. 4 shows the evolutions of PL from two typical ZnO thin films (T_{ph}=300 °C and 500 °C), as a function of *T*. Because of the thermal dissociation of donor-bound excitons, free excitonic emission (FX) located at 3.377 eV are observed at high *T* for both samples. For the film with T_{ph}=300 °C, we note that the PL-intensity of DAP-band and SD-band quench rapidly and are hardly detectable above $T > 40$ K, consistent with the previous finding [23]. Furthermore, the eA°-band persists up to higher *T* and its band-profile starts to deviate from symmetric lineshape. The thermal distribution of electrons involved in the transitions at high *T* results in high-energy asymmetric tails [23], as can be seen in the spectrum measured at 80 K. These observations further confirms the assignment of DAP-, eA°- and SD-transitions. In the film of T_{ph}=300 °C, we also detected spectral blueshift of the small hump (around 3.23 eV) as *T* increases. This is because the LO-phonon-sideband of DAP-emission diminishes as *T* increases. At *T*=15 K, a merged impurity-defect emission from the film of T_{ph}=500 °C is observed, as shown in Fig. 4(b). Similar to the film of T_{ph}=300 °C, the DAP-emission disappears above 40 K and the eA°-emission remains. Therefore, we can conclude that the origin of the impurity-defect emission from the film of T_{ph}=500 °C is nothing else but DAP- and eA°-transitions.

Fig. 5 illustrates the low-*T* PL spectra of the ZnO thin films, recorded at broad spectral range. The near-band-edge (NBE) emission is mainly due to the D°X-transitions mentioned above. The deep level (DL) emissions are attributable to defect-related transitions. The red emission centering around 1.8 eV could be attributed to the transition from oxygen vacancy level to the top of the valence of ZnO [25,26]. Moreover, the transitions between the zinc interstitial and oxygen interstitial may contribute the small hump centering about 2 eV at the DL emission band [26]. The intensity of DL emission increases abruptly as T_{ph} increases from 300 °C to 400 °C. In accordance with the results of XRD and SEM, the vigorous and simultaneous chemical processes at 400 °C induce metastable imperfections in the thin film, which cannot be annihilated by post-annealing treatment. This leads to larger DL emission intensity. These crystalline imperfections reduce as T_{ph} increases to 500 °C, owing to reconstruction of atomic arrangement at the pre-heating stage. Therefore, the DL emission intensity is almost negligible in the thin film with T_{ph}=500 °C. However, the DL emission intensity enhances again in the film with T_{ph}=600 °C because the number of oxygen vacancy increases with increasing T_{ph} [27].

4. Conclusion

In summary, we investigated the structural and low-*T* PL properties of sol–gel derived ZnO thin films, prepared from zinc nitrate solution. The emphasis has been given on the effects of pre-heating temperature on the PL spectra. Especially, the pre-heating crystallization plays an important role in the lineshape of PL spectra. The donor-bound excitonic emission and relatively weak impurity-defect emission characterizes the low-*T* NBE-PL spectra. Deep level emissions due to oxygen vacancies, oxygen interstitials, and zinc interstitials are detected at orange-to-red spectral region. As pre-heating temperature reaches 400 °C, vaporization

of organic residuals and thermal decomposition of zinc nitrate happens abruptly and simultaneously, leading to random oriented growth of films, larger degree of porosity, change in lineshape of impurity-defect emission, and enhancement of deep-level emission intensity. Further increase in pre-heating temperature enables rearrangement of atoms at the pre-heating stage, leading to *c*-axis oriented growth of films, further modification in lineshape of impurity-defect emission, and reduction of deep-level emission intensity.

Acknowledgement

This research was supported by National Science Council of Taiwan under Grant No. NSC-99-2112-M-390-001-MY3.

References

[1] Ü. Özgür, Ya.I. Alivov, C. Liu, A. Teke, M.A. Reshchikov, S. Doğan, A. Avrutin, S.-J. Cho, H. Morkoč, J. Appl. Phys. 98 (2005) 041301.
[2] Z.K. Tang, G.K.L. Wong, P. Yu, M. Kawasaki, A. Ohtomo, H. Koinuma, Y. Segawa, Appl. Phys. Lett. 72 (1998) 3270.
[3] X. Ma, P. Chen, D. Li, Y. Zhang, D. Yang, Appl. Phys. Lett. 91 (2007) 251109.
[4] W.J. Jeong, S.K. Kim, G.C. Park, Thin Solid Films506–507 (2006) 180.
[5] D. Gupta, M. Anand, S.W. Ryu, Y.K. Choi, S. Yoo, Appl. Phys. Lett. 93 (2008) 224106.
[6] S.T. Shishiyanu, T.S. Shishiyanu, O.I. Lupan, Sens. Actuators, B 107 (2005) 379.
[7] S. Krishnamoorthy, A.A. Iliadis, Solid State Electron. 52 (2008) 1710.
[8] M. Zamfirescu, A. Kavokin, B. Gil, G. Malpuech, M. Kaliteevski, Phys. Rev. B: Condens. Matter 65 (2002) 161205.
[9] R. Shimada, J. Xie, V. Avrutin, Ü. Özgür, H. Morkoč, Appl. Phys. Lett. 92 (2008) 011127.
[10] X. Chen, K. Ruan, G. Wu, D. Bao, Appl. Phys. Lett. 93 (2008) 112112.
[11] M. Ohyama, H. Kozuka, T. Yoko, Thin Solid Films 306 (1997) 78.
[12] Y.S. Kim, W.P. Tai, S.J. Shu, Thin Solid Films 491 (2005) 153.
[13] A.M.P. Santos, Edval J.P. Santos, Thin Solid Films 516 (2008) 6210.
[14] L. Znaidi, Mater. Sci. Eng., B 174 (2010) 18.
[15] T. Ehara, T. Otsuki, J. Abe, T. Ueno, M. Ito, T. Hirayama, Phys. Status Solidi A 206 (2009) 2139.
[16] R. Brenier, L. Ortéga, J. Sol-Gel Sci. Technol. 29 (2004) 137.
[17] J. Petersen, C. Brimont, M. Gallart, O. Crégut, G. Schmerber, P. Gilliot, B. Hönerlage, C. Ulhaq-Bouillet, J.L. Rehspringer, C. Leuvrey, S. Colis, H. Aubriet, C. Becker, D. Ruch, A. Slaoui, A. Dinia, J. Appl. Phys. 104 (2008) 113539.
[18] P. Sagar, P.K. Shishodia, R.M. Mehra, H. Okada, A. Wakahara, A. Yoshida, J. Lumin. 126 (2007) 800.
[19] S. Mandal, M.L.N. Goswami, K. Das, A. Dhar, S.K. Ray, Thin Solid Films 516 (2008) 8702.
[20] N. Kumar, R. Kaur, R.M. Mehra, J. Lumin. 126 (2007) 784.
[21] first ed.,J.C. Bailar, A.F. Trotman-Dickenson, H.J. Emeleus, S.R. Nyholm (Eds.), Pergamon, Oxford, 1973.
[22] B.K. Meyer, H. Alves, D.M. Hoffmann, W. Kriegseis, D. Forster, F. Bertram, J. Christen, A. Hoffmann, M. Straßburg, M. Dworzak, U. Haboeck, A.V. Rodina, Phys. Status Solidi B 241 (2004) 231.
[23] M. Schirra, R. Schneider, A. Reiser, G.M. Prinz, M. Feneberg, J. Biskupek, U. Kaiser, C.E. Krill, K. Thonke, R. Sauer, Phys. Rev. B: Condens. Matter 77 (2008) 125215.
[24] D. Tainoff, B. Masenelli, P. Mélinon, A. Belsky, G. Ledoux, D. Amans, C. Dujardin, N. Ferodov, P. Martin, Phys. Rev. B: Condens. Matter 81 (2010) 115304.
[25] C.H. Ahn, Y.Y. Kim, D.C. Kim, S.K. Mohanta, H.K. Cho, J. Appl. Phys. 105 (2009) 013502.
[26] N.H. Alvi, K. Ul Hasan, O. Nur, M. Willander, Nanoscale Res. Lett. 6 (2011) 130.
[27] H.S. Kang, J.S. Kang, J.W. Kim, S.Y. Lee, J. Appl. Phys. 95 (2004) 1246.